Neuron, Volume *99*

Supplemental Information

The Innate Immune Receptors TLR2/4 Mediate Repeated Social Defeat Stress-Induced Social Avoidance through Prefrontal Microglial Activation

Xiang Nie, Shiho Kitaoka, Kohei Tanaka, Eri Segi-Nishida, Yuki Imoto, Atsubumi Ogawa, Fumitake Nakano, Ayaka Tomohiro, Kazuki Nakayama, Masayuki Taniguchi, Yuko Mimori-Kiyosue, Akira Kakizuka, Shuh Narumiya, and Tomoyuki Furuyashiki

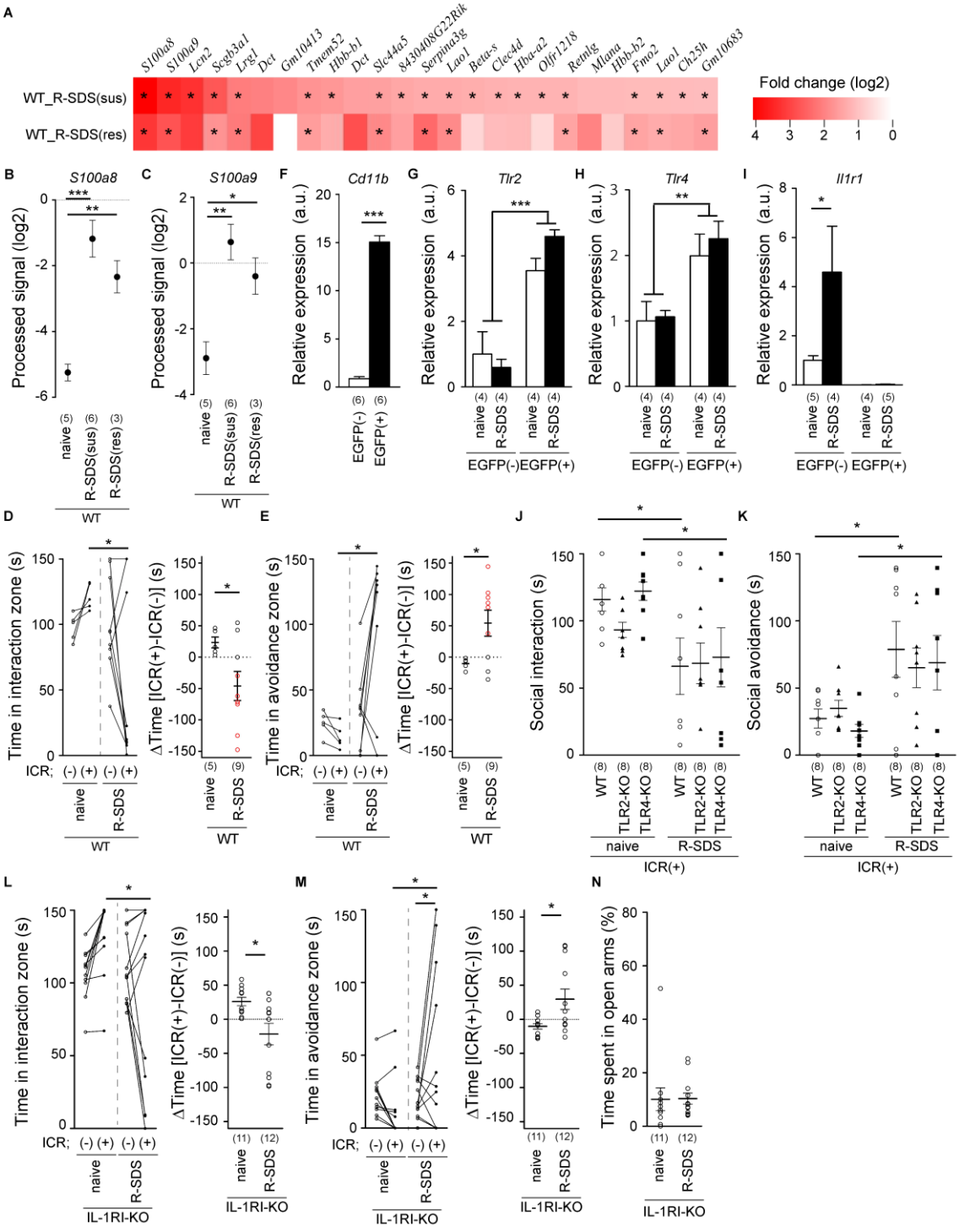

Figure S1, related to Figures 1 and 2.

Behavioral and gene expression analyses of TLR2, TLR4, and IL-1RI

(A) A heat map showing R-SDS-induced changes in gene expression of the top 25 most upregulated genes in the mPFC from susceptible and resilient wild-type mice ("WT_R-SDS(sus)" and "WT_R-SDS(res)",

respectively). *P<0.05 for unpaired *t*-test for the changes in gene expression for the indicated probes. (**B** and **C**) The expression levels of S100A8 (**B**) and S100A9 (**C**) in the mPFC of susceptible and resilient wild-type mice ("R-SDS(sus)" and "R-SDS(res)", respectively) at 4 h after R-SDS as well as wild-type mice without SDS ("naïve"). *P<0.05, **P<0.01, ***P<0.001 for Bonferroni's multiple comparison test. (**D** and **E**) The durations for presence in the interaction (**D**) or avoidance (**E**) zone without and with an ICR mouse and the differences between these durations without and with an ICR mouse (ΔTime [ICR(+)-ICR(-)]), for wild-type mice ("WT") with or without prior R-SDS ("R-SDS" and "naïve"). Red dots in right panels indicate the data from susceptible mice. *P<0.05 for Bonferroni's multiple comparison test (left panels) or unpaired *t*-test (right panels). (**F**-**I**) mRNA levels of CD11b (**F**), TLR2 (**G**), TLR4 (**H**) and IL-1RI (**I**) in EGFP-positive cells ("EGFP(+)") and EGFP-negative cells ("EGFP(-)") isolated from CX3CR1-EGFP mice, in which EGFP is selectively expressed in microglia and monocytes (a minor population) in the brain, with or without prior R-SDS ("R-SDS" or "naïve", respectively). The levels were normalized to that of β-actin to minimize sample variance. The levels were further normalized to those of the control groups, namely EGFP(-) in Figure S1F and naïve EGFP(-) in Figure S1G-I, and are shown. ***P<0.001 for unpaired *t*-test (**F**) and *P<0.05 for Bonferroni's multiple comparison test (**I**). (**J** and **K**) The durations for presence in the interaction (**J**) or avoidance (**K**) zone with an ICR mouse for wild-type mice (WT), TLR2-KO mice, and TLR4-KO mice before and after R-SDS ("naïve" and "R-SDS", respectively). The same individuals were analyzed and statistically compared before and after R-SDS. *P<0.05 for Bonferroni's multiple comparison test. (**L** and **M**) The durations within the interaction (**L**) or avoidance (**M**) zone without and with an ICR mouse and the differences between these durations without and with an ICR mouse (ΔTime [ICR(+)-ICR(-)]) in IL-1RI-KO mice with or without prior R-SDS ("R-SDS" or "naïve", respectively). *P<0.05 for Bonferroni's multiple comparison test (left panels) or unpaired *t*-test (right panels). (**N**) The level of anxiety of IL-1RI-KO mice with or without prior R-SDS ("R-SDS" or "naïve", respectively). The proportion of the time spent in the open arms in the elevated plus maze was measured as an index of anxiety. The number of mice is shown below each group. Data are shown as means ± SEM.

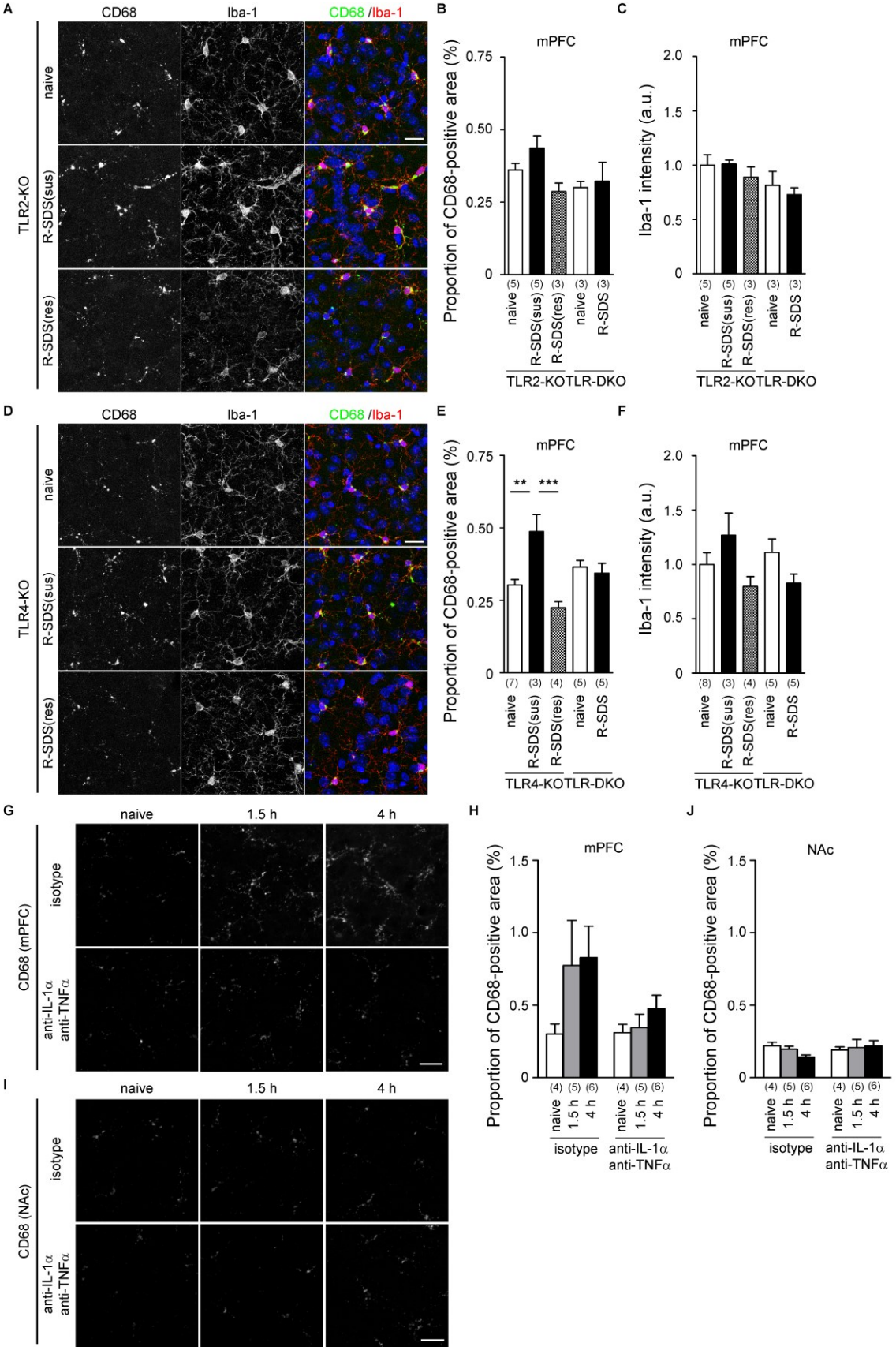
A
CD68
Iba-1
CD68 /Iba-1
TLR2-KO
naive
R-SDS(sus)
R-SDS(res)
B
mPFC
Proportion of CD68-positive area (%)
0.75
0.50
0.25
0
(5) (5) (3) (3) (3)
naive
R-SDS(sus)
R-SDS(res)
naive
R-SDS
TLR2-KO
TLR-DKO
C
mPFC
Iba-1 intensity (a.u.)
2.0
1.5
1.0
0.5
0
(5) (5) (3) (3) (3)
naive
R-SDS(sus)
R-SDS(res)
naive
R-SDS
TLR2-KO
TLR-DKO
D
CD68
Iba-1
CD68 /Iba-1
TLR4-KO
naive
R-SDS(sus)
R-SDS(res)
E
mPFC
Proportion of CD68-positive area (%)
**
***
0.75
0.50
0.25
0
(7) (3) (4) (5) (5)
naive
R-SDS(sus)
R-SDS(res)
naive
R-SDS
TLR4-KO
TLR-DKO
F
mPFC
Iba-1 intensity (a.u.)
2.0
1.5
1.0
0.5
0
(8) (3) (4) (5) (5)
naive
R-SDS(sus)
R-SDS(res)
naive
R-SDS
TLR4-KO
TLR-DKO
G
naive
1.5 h
4 h
CD68 (mPFC)
isotype
anti-IL-1α
anti-TNFα
H
mPFC
Proportion of CD68-positive area (%)
1.5
1.0
0.5
0
(4) (5) (6) (4) (5) (6)
naive
1.5 h
4 h
naive
1.5 h
4 h
isotype
anti-IL-1α
anti-TNFα
I
naive
1.5 h
4 h
CD68 (NAc)
isotype
anti-IL-1α
anti-TNFα
J
NAc
Proportion of CD68-positive area (%)
1.5
1.0
0.5
0
(4) (5) (6) (4) (5) (6)
naive
1.5 h
4 h
naive
1.5 h
4 h
isotype
anti-IL-1α
anti-TNFα

Figure S2, related to Figures 3 and 8.

TLR2 and TLR4 deficiency attenuates R-SDS-induced activation of mPFC microglia

(**A**-**F**) Representative images (**A** and **D**) and quantitative analyses (**B**, **C**, **E** and **F**) of immunostaining for CD68 and Iba-1 in the mPFC of TLR2-KO mice (**A**-**C**) and TLR4-KO mice (**D**-**F**) without SDS ("naïve"), susceptible and resilient mice ("R-SDS(sus)" and R-SDS(res)", respectively) with the respective genotypes, and TLR-DKO littermates (**B**, **C**, **E** and **F**) with or without R-SDS ("R-SDS" and "naïve", respectively) at 1.5 h after the last session of R-SDS. The images from TLR-DKO littermates are not shown in this figure, since these images are similar to those from TLR-DKO mice shown in Figure 3A and 3C. In the merged images, CD68 and Iba-1 signals are shown in green and red, respectively. CD68 signals in Iba-1 positive microglia are seen in yellow. Nuclei were counterstained with Hoechst 33342 and are shown in blue. The values of Iba-1 intensity were normalized to that of naïve TLR2-KO or TLR4-KO mice for Figure S2C or S2F, respectively. (**G**-**J**) Representative images (**G** and **I**) and quantitative analyses (**H** and **J**) of immunostaining of CD68 in the mPFC (**G** and **H**) and NAc (**I** and **J**) of wild-type mice which received mPFC infusions with a mixture of neutralizing antibodies for IL-1α and TNFα ("anti-IL-1α anti-TNFα") or control antibodies of the corresponding isotypes ("isotype") without SDS ("naïve"), and at 1.5 h and 4 h after the last session of a shorter version of R-SDS (see Figure 8A). Scale bars, 20 μm. $^{**}P<0.01$, $^{***}P<0.001$ for Bonferroni's multiple comparison test. The number of mice is shown below each group. Data are shown as means ± SEM.

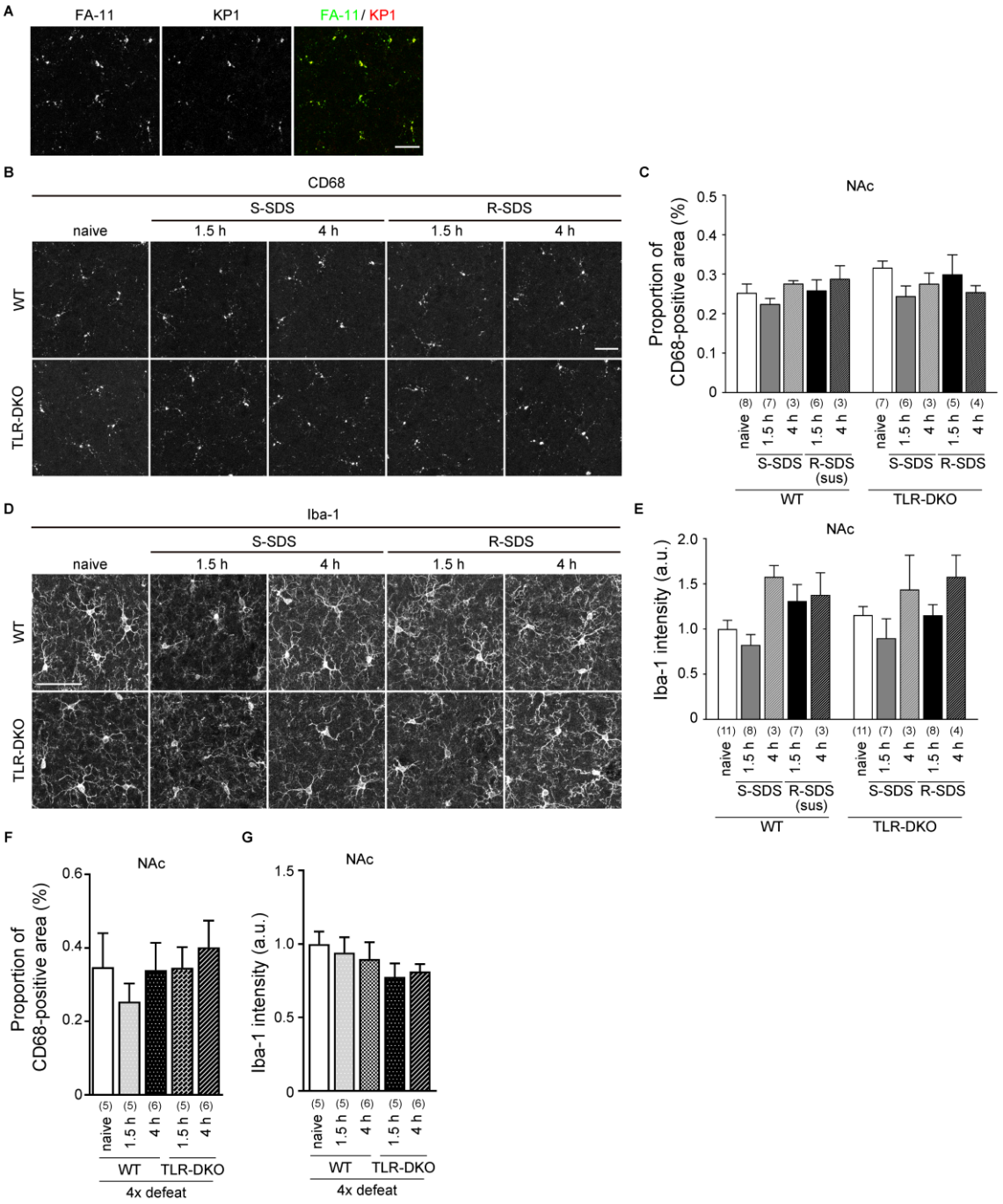

Figure S3, related to Figure 3.

R-SDS does not induce activation of NAc microglia in wild-type mice or TLR-DKO mice

(**A**) Colocalization of CD68 signals with FA-11, a monoclonal anti-CD68 antibody which was mainly used in this study, and those with KP1, another monoclonal anti-CD68 antibody. This colocalization with the two independent antibodies confirmed the specificity of CD68 signals. Scale bar, 50 μm. (**B**-**E**) Representative images (**B** and **D**) and quantitative analyses (**C** and **E**) of CD68 (**B** and **C**) and Iba-1 (**D** and

E) immunostaining in the NAc of wild-type mice (WT) and TLR-DKO mice without SDS ("naïve"), and at 1.5 h and 4 h after S-SDS and the last session of R-SDS. For wild-type mice after R-SDS, the images were taken and analyzed only from susceptible mice ("R-SDS(sus)"). Scale bars, 50 μm. (**F** and **G**) Quantitative analyses of CD68 (**F**) and Iba-1 (**G**) immunostaining in the NAc of wild-type mice (WT) and TLR-DKO mice without SDS ("naïve") and at 1.5 h and 4 h after the last session of R-SDS for 4 days ("4× defeat"). The values of Iba-1 intensity were normalized to that of naïve wild-type mice. The number of mice is shown below each group. Data are shown as means ± SEM.

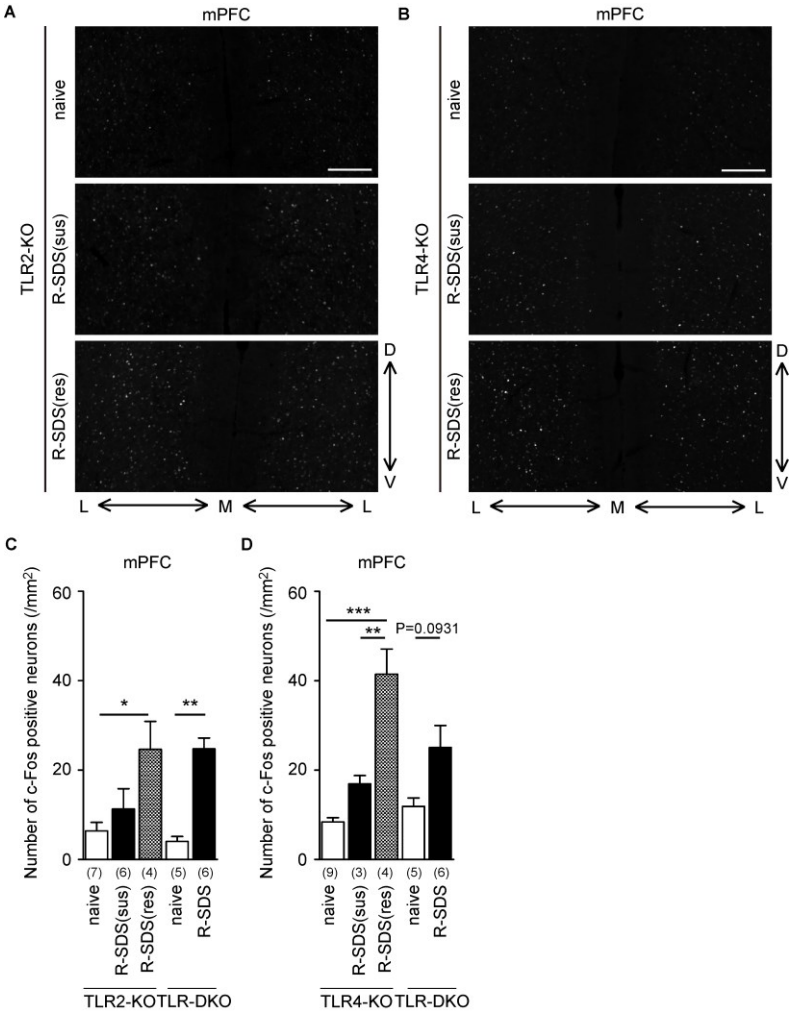

Figure S4, related to Figure 5.

SDS-induced c-Fos expression in mPFC neurons of TLR2-KO mice and TLR4-KO mice as well as TLR-DKO littermates

Representative images (**A** and **B**) and quantitative analyses (**C** and **D**) of c-Fos immunostaining in mPFC of TLR2-KO mice (**A** and **C**) and TLR4-KO mice (**B** and **D**) without SDS ("naïve"), susceptible and resilient mice ("R-SDS(sus)" and "R-SDS(res)", respectively) of the respective genotypes, and TLR-DKO mice (**C** and **D**) with or without R-SDS ("R-SDS" and "naïve", respectively) at 1.5 h after the last session of R-SDS. The images from TLR-DKO littermates are not shown in this figure, since these images are similar to those from TLR-DKO mice shown in Figure 5B. The orientations of the images are indicated by arrows (L, lateral; M, medial; D, dorsal; V, ventral). Scale bars, 100 μm. **P*<0.05, ***P*<0.01, ****P*<0.001 for Bonferroni's multiple comparison test. The number of mice is shown below each group. Data are shown as means ± SEM.

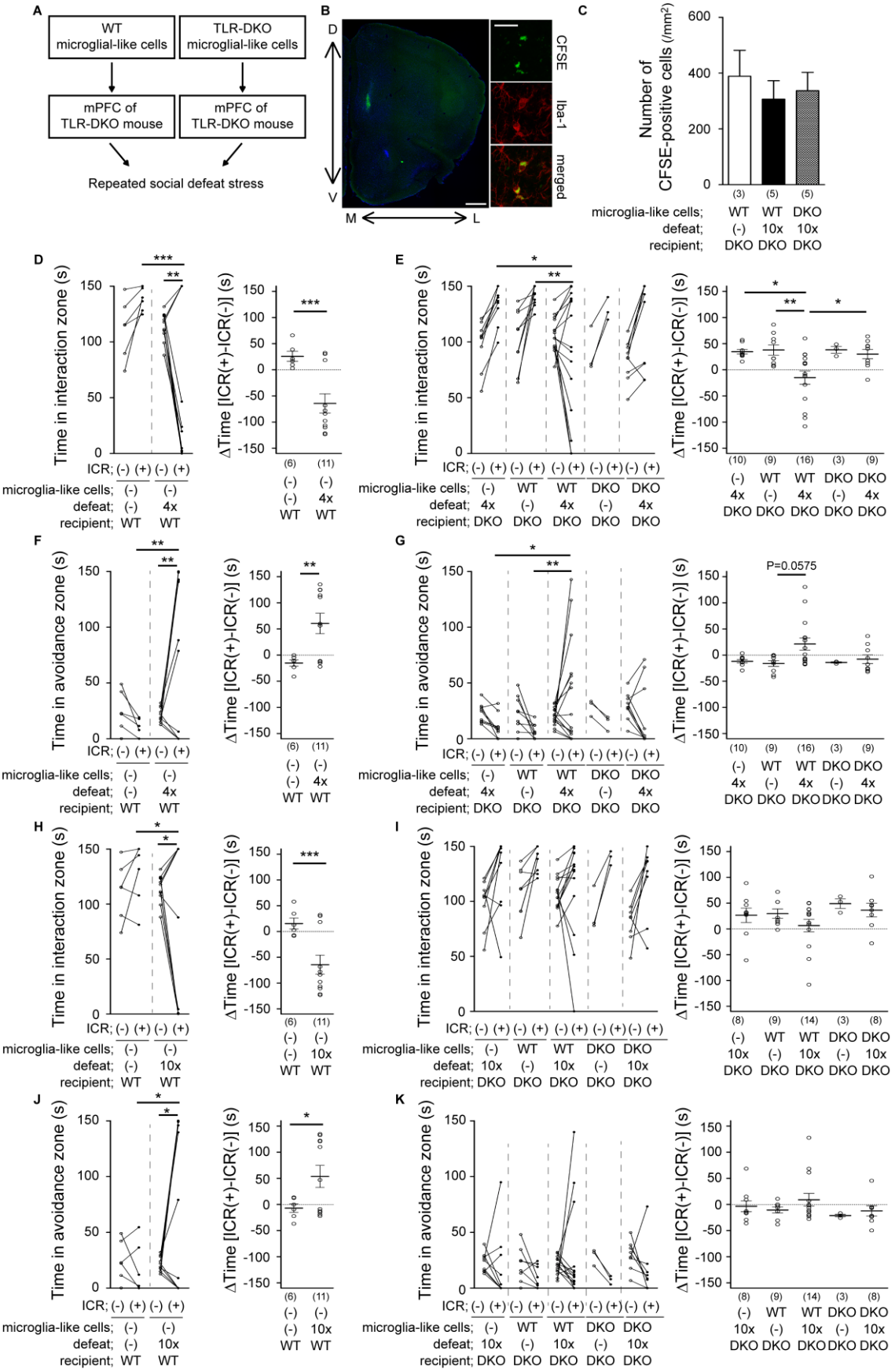
A
WT microglial-like cells
TLR-DKO microglial-like cells
mPFC of TLR-DKO mouse
mPFC of TLR-DKO mouse
Repeated social defeat stress
B
D
V
M
L
CFSE
Iba-1
merged
C
Number of CFSE-positive cells (/mm2)
microglia-like cells; WT WT DKO
defeat; (-) 10x 10x
recipient; DKO DKO DKO
D
Time in interaction zone (s)
ΔTime [ICR(+)-ICR(-)] (s)
microglia-like cells; (-) (-)
defeat; (-) 4x
recipient; WT WT
E
microglia-like cells; (-) WT WT DKO DKO
defeat; 4x (-) 4x (-) 4x
recipient; DKO DKO DKO DKO DKO
F
Time in avoidance zone (s)
G
P=0.0575
H
Time in interaction zone (s)
microglia-like cells; (-) (-)
defeat; (-) 10x
recipient; WT WT
I
microglia-like cells; (-) WT WT DKO DKO
defeat; 10x (-) 10x (-) 10x
recipient; DKO DKO DKO DKO DKO
J
Time in avoidance zone (s)
K

Figure S5, related to Figure 6.

Transplantation of wild-type microglia-like cells into the mPFC of TLR-DKO mice transiently restores social avoidance induced by R-SDS

(**A**) Design of behavioral experiments with transplantation of microglia-like cells. Primary microglia-like cells were obtained from wild-type (WT) and TLR-DKO neonates, and were transplanted to the mPFC of TLR-DKO mice. After a four-week recovery, the mice were subjected to R-SDS. (**B**) Representative images of transplanted microglia-like cells in the mPFC. Wild-type microglia-like cells were labeled with CFSE and locally infused into the mPFC of TLR-DKO mice. Fluorescence images were taken after the four-week recovery. Microglia were visualized by Iba-1 staining. CFSE and Iba-1 signals are shown in green and red, respectively. Nuclei counterstained with Hoechst 33342 are shown in blue. The orientations of the images are indicated by arrows (L, lateral; M, medial; D, dorsal; V, ventral). Scale bars, 500 μm and 25 μm for the lower and higher magnifications, respectively. (**C**) The numbers of CFSE-positive cells in TLR-DKO mice that received transplantation of wild-type (WT) or TLR-DKO (DKO) microglia-like cells into the mPFC with or without prior R-SDS for 10 days ("10×" or "(-)", respectively). (**D**-**K**) The durations for presence in the interaction (**D**, **E**, **H** and **I**) or avoidance (**F**, **G**, **J** and **K**) zone without and with an ICR mouse and the differences between these durations without and with an ICR mouse (ΔTime [ICR(+)-ICR(-)]) in wild-type recipient mice (WT) that received a sham operation ("(-)") (**D**, **F**, **H** and **J**), and in TLR-DKO recipient mice which received a sham operation ("(-)"), or transplantation of wild-type (WT) or TLR-DKO (DKO) microglia-like cells into the mPFC (**E**, **G**, **I** and **K**) with or without prior R-SDS for 4 days ("4×" or "(-)", respectively; **D**-**G**) or for 10 days ("10×" or "(-)", respectively; **H**-**K**). n.s. (not significant), **P*<0.05, ***P*<0.01, ****P*<0.001 for unpaired *t*-test for pairwise comparisons, or for Bonferroni's multiple comparison test for comparisons among more than two groups. The number of mice is shown below each group. Data are shown as means ± SEM.

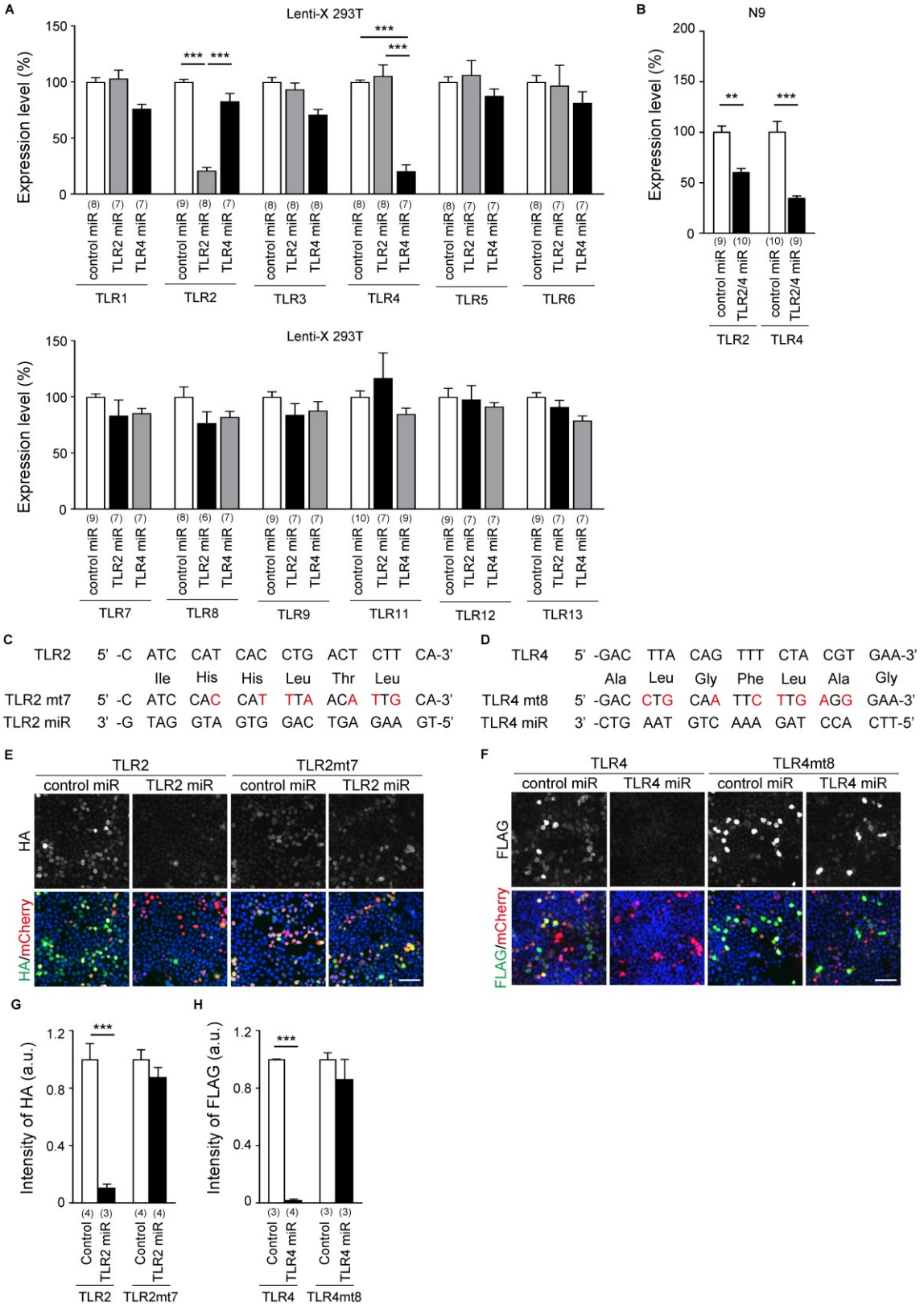
A
Lenti-X 293T
Expression level (%)
control miR
TLR2 miR
TLR4 miR
TLR1
TLR2
TLR3
TLR4
TLR5
TLR6
Lenti-X 293T
TLR7
TLR8
TLR9
TLR11
TLR12
TLR13
B
N9
control miR
TLR2/4 miR
TLR2
TLR4
C
TLR2 5' -C ATC CAT CAC CTG ACT CTT CA-3'
Ile His His Leu Thr Leu
TLR2 mt7 5' -C ATC CAC CAT TTA ACA TTG CA-3'
TLR2 miR 3' -G TAG GTA GTG GAC TGA GAA GT-5'
D
TLR4 5' -GAC TTA CAG TTT CTA CGT GAA-3'
Ala Leu Gly Phe Leu Ala Gly
TLR4 mt8 5' -GAC CTG CAA TTC TTG AGG GAA-3'
TLR4 miR 3' -CTG AAT GTC AAA GAT CCA CTT-5'
E
TLR2
TLR2mt7
control miR
TLR2 miR
HA
HA/mCherry
F
TLR4
TLR4mt8
TLR4 miR
FLAG
FLAG/mCherry
G
Intensity of HA (a.u.)
Control
TLR2mt7
H
Intensity of FLAG (a.u.)
TLR4mt8

Figure S6, related to Figure 6.

TLR2/4 microRNA selectively suppresses mRNA expression of TLR2 and TLR4 *in vitro*

(**A**) RNA interference with TLR2 or TLR4 microRNA efficiently and specifically suppresses mRNA expression of the corresponding TLR isoform in Lenti-X 293T cells. Various mouse TLR isoforms (TLR1 to TLR13) were overexpressed with TLR2 or TLR4 microRNA (miR) as well as control microRNA, and their expression levels were quantified by real-time RT-PCR. ***P<0.001 for Bonferroni's multiple comparison test. (**B**) Lentivirus-delivered TLR2/4 microRNA, in which TLR4 microRNA and TLR2 microRNA are tandemly connected, simultaneously suppressed endogenous mRNA expression of TLR2 and TLR4 in the N9 microglial cells. The values were normalized to those with control microRNA. **P<0.01, ***P<0.001 for unpaired t-test. (**C** and **D**) DNA sequences for microRNA-targeting regions of TLR2 (**C**) and TLR4 (**D**) and the corresponding regions of microRNA-resistant mutant cDNAs of these genes ("TLR2mt7" and "TLR4mt8", respectively) with no change in the amino acid sequences. Mutations in these mutants are highlighted in red. (**E** and **F**) Representative images of immunostaining for TLR2 (**E**), TLR4 (**F**) or the respective microRNA-resistant mutants ("TLR2mt7" and "TLR4mt8") with the corresponding microRNA or control microRNA in Lenti-X 293T cells. TLR2 and TLR2mt7 cDNAs were tagged with HA and detected by HA immunostaining. TLR4 and TLR4mt8 cDNAs were tagged with FLAG and detected by FLAG immunostaining. mCherry was simultaneously expressed with TLR2 or TLR4 microRNA to identify cells expressing these miRNAs. HA or FLAG signals and mCherry are shown in green and red, respectively, in the merged images. Nuclear counterstaining with Hoechst 33342 is shown in blue. Scale bars, 25 μm. (**G** and **H**) The fluorescent intensities of HA (**G**) and FLAG (**H**) tags in the experimental conditions shown in **E** and **F**, respectively. The values were normalized to those with control microRNA. ***P<0.001 for unpaired t-test. The number of analyzed wells is shown below each group. Data are shown as means ± SEM.

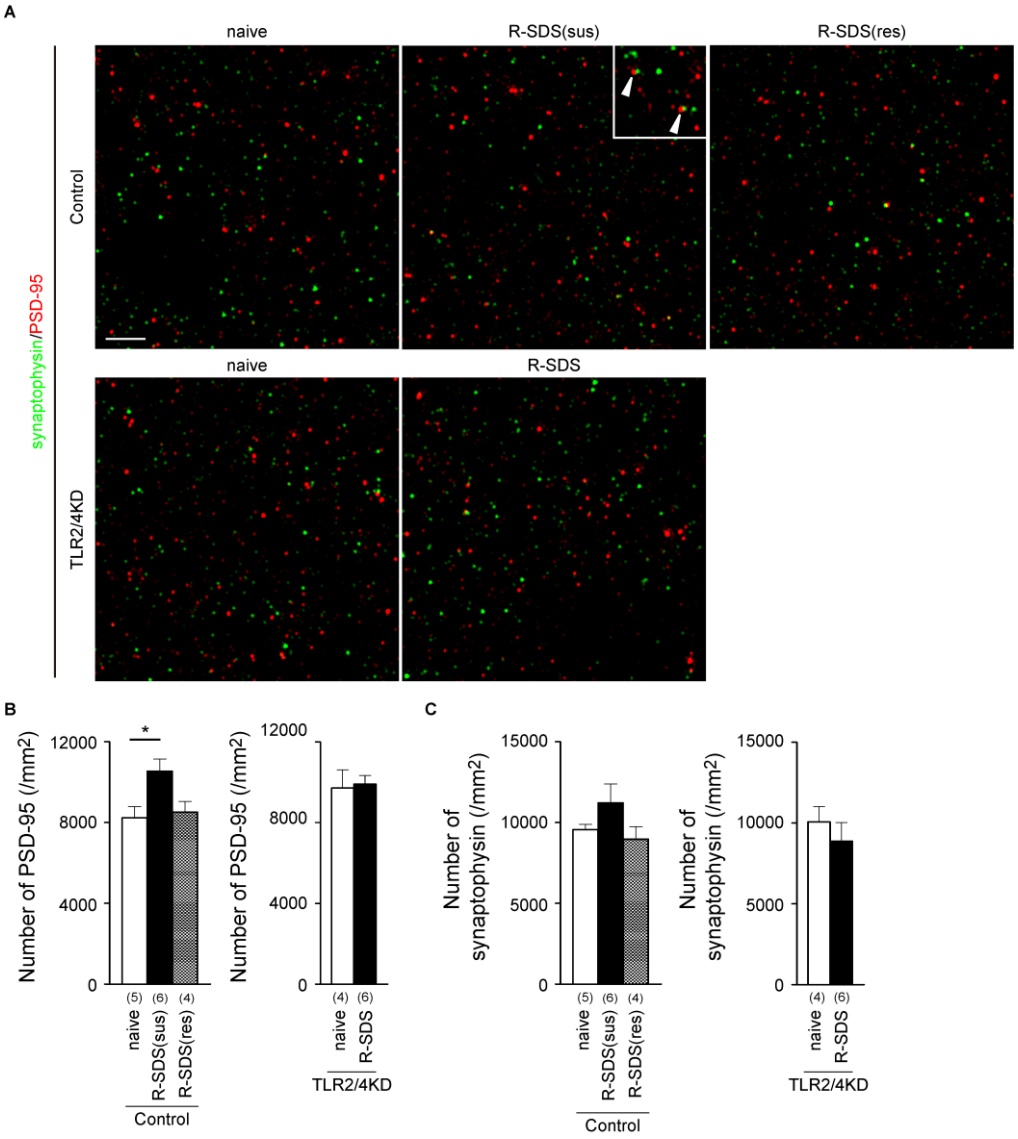

Figure S7, related to Figure 6.

R-SDS increases the number of PSD-95-positive puncta in the mPFC in a manner dependent on TLR2/4 expressed in mPFC microglia

Representative SIM images (**A**) and quantitative analyses (**B** and **C**) of immunostaining for synaptophysin (green in **A**) and PSD-95 (red in **A**) in the deep layer of the mPFC of CX3CR1-CreER mice that received mPFC injections of lentiviral vectors expressing control microRNA ("Control") or TLR2/4 microRNA ("TLR2/4KD"). The images were taken from susceptible and resilient CX3CR1-CreER mice ("R-SDS(sus)" and "R-SDS(res)", respectively) expressing control microRNA, and those expressing TLR2/4 microRNA ("R-SDS") at 1.5 h after R-SDS, as well as those expressing control or TLR2/4 microRNA without R-SDS ("naïve"). Arrowheads in **A** indicate the juxtaposition of synaptophysin and PSD-95 punctate signals reminiscent of excitatory synapses. Scale bar, 5 μm. **P*<0.05 for Bonferroni's multiple comparison test.

The number of mice is shown below each group. Data are shown as means ± SEM.

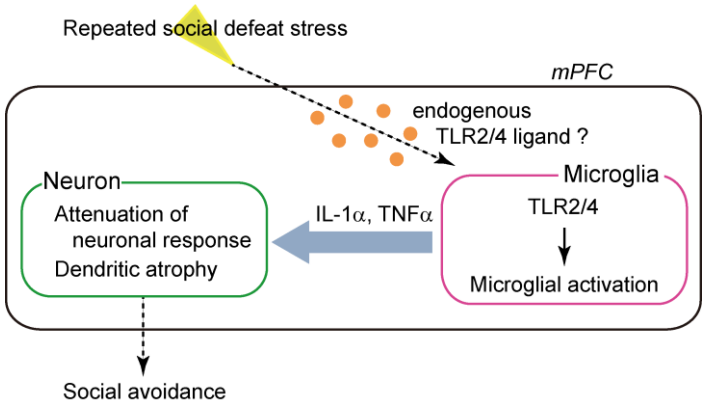

Figure S8, related to all Figures.

The role of TLR2/4 in mPFC microglia for R-SDS-induced neuronal and behavioral changes

Our findings demonstrate that R-SDS induces activation of mPFC microglia through TLR2/4 for neuronal and behavioral changes, although the endogenous TLR2/4 ligand for this microglial activation remains to be identified. We also suggest that IL-1α and TNFα derived from the activated mPFC microglia mediate neuronal response attenuation and dendritic atrophy in the mPFC, thereby leading to social avoidance.